Energy saving potential with smart thermostats in low-energy homes in cold climate

Tuule Mall Kull[1,*], *Karl-Rihard* Penu[1], *Martin* Thalfeldt[1], and *Jarek* Kurnitski[1,2]

[1]Nearly Zero Energy Buildings Research Group, Tallinn University of Technology, Ehitajate tee 5, 19086 Tallinn, Estonia
[2]Department of Civil Engineering, Rakentajanaukio 4 A, Aalto University, FI-02150 Espoo, Finland

Abstract. Smart home systems with smart thermostats have been used for years. Although initially mostly installed for improving comfort, their energy saving potential has become a renowned topic. The main potential lies in temperature reduction during the times people are not home, which can be detected by positioning their phones. Even if the locating is precise, the maximum time people are away from home is short in comparison to the buildings' time constants. The gaps are shortened by the smart thermostats, which start to heat up hours before occupancy to ensure comfort temperatures at arrival, and low losses through high insulation and heat-recovery ventilation in new buildings, which slow down the cool-down process additional to the thermal mass. Therefore, it is not clear how high the actual savings can be for smart thermostats in new buildings. In this work, a smart radiator valve was installed for a radiator in a test building. Temperature setback measurements were used to calibrate a simulation model in IDA ICE. A simulation analysis was carried out for estimating the energy saving potential in a cold climate for different usage profiles.

1 Introduction

Smart thermostats including programmable setpoints and learning of heat-up time have been used for a decade already. Still, energy saving has not been in the top interests of the users [1]. However, with very energy-efficient buildings and people's awareness, the topic has become more important.

Many smart home providers advertise energy savings as they locate the owners by their smartphones and switch off the heating when there is no one home [2]. When the owners approach home, the heating turns on again. This means that the savings heavily depend on the behavior of the people. It has been also analyzed how to change their behavior for more energy savings.

However, even if the people behave predictably, the nearly zero energy buildings cool down extremely slowly and therefore, the saving potential can be limited. Especially if the thermostat has to heat up the building for the arrival of the occupant, reducing the free-float times even more.

Another restriction for the energy saving in multi-room dwellings is the difference in usage and setpoint profiles between the rooms. When a room is not heated, the adjacent rooms are heated more and the overall energy consumption does not change much. If we use the same profile for the whole house, the gaps when heating is not needed are shorter and the time often overlaps with solar gains for residential buildings. This is the period when heating is not often needed in the low energy buildings due to high influence of solar gains and therefore the savings are small. The energy savings can be clearly larger when lower temperatures are allowed during nighttime.

In this work, the energy saving potential for a set of different setpoint and internal heat profiles is estimated in a energy-efficient building. The results are based on simulations on a calibrated model of room, radiator and smart thermostat.

2 Methods

The study consisted of four main parts shown in Fig. 1:
- Measurements in a test house,
- Building model calibration in IDA ICE 4.8 SP1 [3],
- Simulations for energy savings of one room,
- Simulations for energy savings in a small residential house.

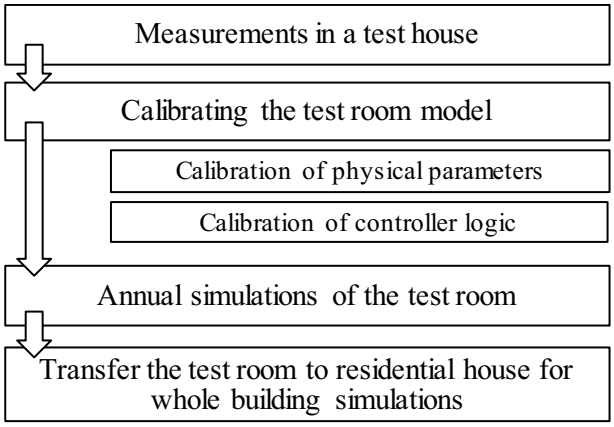

Fig. 1. Flow chart of the applied methodology

* Corresponding author: tuule.kull@taltech.ee

2.1. Measurements

The aim of the physical experiment was to gather input data for room and radiator model calibration at changing setpoint (*Tset*) as well as to estimate how a smart home thermostat could work. The experiment was carried out during a 13-day period in February 2020, including 9 weekdays and 4 weekend days. It was performed in a test house at TalTech university campus in Tallinn, Estonia. The building has one floor with 100 m^2 and an unheated attic space fully open to the inner corridor. The external walls and the roof are wooden frame construction, under the concrete floor there is crawlspace. The U-values of the constructions are the following: external walls 0.12, windows 0.75, roof and floor 0.08 W/(m^2K).

The measurements were carried out in one test room shown in Fig. 2, the measurement points are shown in red circles. The room area is 10.4 m^2; it has two 4-m^2 windows, one toward south and the other facing west. The air temperature (*Tair*) was measured in the centre and in the corner of the room at 1-m height. The air temperatures were also measured in the adjacent rooms. The door to test room 8 in the east was insulated with 50-mm insulation board and taped for air-tightness. The southern wall has through-wall test ventilation units, which were also taped. The ventilation was turned off and the valves taped.

The test room was heated with one floor-connected type-11 hydraulic radiator, 1.2 m long and 0.3 m high with nominal power of 263 W. The radiator was equipped with a smart thermostat. Three temperature sensors were installed on the radiator surface. The supply and return temperatures (*Tsup* and *Tret*, blue and orange circle in Fig. 2) were measured on the external surface of the supply and return pipes between the floor and the radiator in the room.

An air-to-water heat pump prepares the supply temperature for the radiators in this test house. The set supply temperature was an outdoor temperature compensated heating curve with 45°C at -10°C, 39°C at 0°C and 31°C at 10°C. All the other radiator circuits were closed from the collector so the mass flow could have been measured at the mixing station. The pump at the mixing station was set to a constant power mode of lowest level possible. The distance from the mixing valve to the measured radiator is almost 10 m.

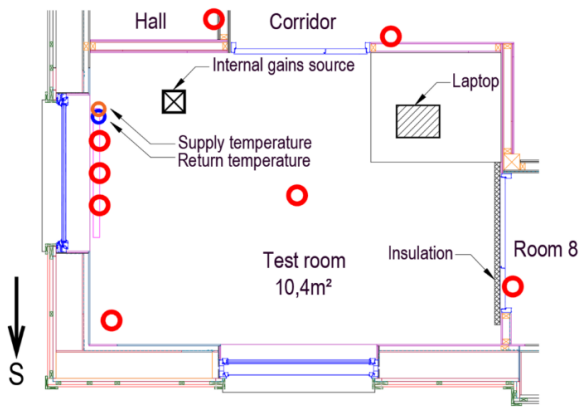

Fig. 2. Test room floor plan with sensor locations (red circles), orange and blue circles note the location of supply and return temperature sensors

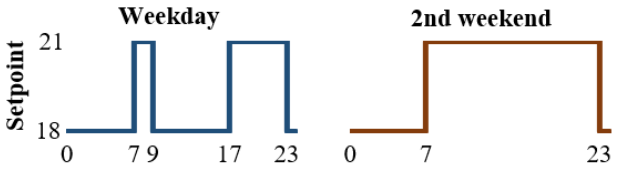

Fig. 3. Temperature setpoint of the smart thermostat during the weekdays and the second weekend, during the first weekend, the setpoint was constantly on 21°C

During the 13-day long experiment, the smart thermostat of the radiator had a variable setpoint shown in Fig. 3. Additional heat was generated by a 90-W internal heat gains source, which emulated a person. During the weekdays it turned on at 5 p.m. and off at 9 a.m. During the weekends, it heated the whole 24 hours. A laptop was on the table, emitting heat at about 13 W constantly. Both devices were plugged into smart sockets and therefore the dynamic emission powers are known.

The weather data was measured locally on the roof of the test house. Air temperature (Tout) measurements as well as diffuse and global irradiation on horizontal were available. The direct solar irradiation was calculated as the difference of the two latter measurements. It was also converted to direct normal irradiation using the solar elevation angles from the IDA ICE software.

2.2 Model calibration and adaption

A simulation model of the test house was calibrated in IDA ICE 4.8 SP1. The model has been previously calibrated for different experiment setups [4–6]. Therefore, the constructions were assumed to be already valid.

The calibration was done in two steps. Initially, measurements from the physical experiment were used wherever possible to determine some unknown parameters of the room and the radiator. Secondly, the unknown logic of the commercial smart thermostat was emulated. The aim was to find a logic that results in energy consumption as similar as possible to the measured case.

2.2.1 Room and radiator calibration

The physical parameters in the test house, which still needed calibrating, were all the leaks from the test room to other rooms and outside, dirtiness of the windows and the transparency of the trees in the park. Time constant and the convection-radiation split of the internal gains were also adapted.

A mathematical optimum was not needed for our application, so the suitable parameter values were found by trial and error of logical parameter value ranges and noting tendencies to choose next combinations. Several parameters were varied simultaneously and several iterations were done before the final parameter values were fixed.

In the calibration model, the measured weather data was used. Also, air temperatures in the adjacent rooms were enforced by using ideal heaters and coolers. In the test room, the input parameter was the supply

temperature. The radiator mass flow was controlled by a proportional-integral (PI) controller, which attempted to follow the measured return temperature. The measured mass flows, radiator surface temperatures and air temperatures in the room were used only for comparison. The main aim was to get the average absolute integrated error (AAE) between the measured and simulated air temperatures minimal, as this determines the heat losses from the room.

Finally, the radiator parameters were varied to get the mass flows to match.

2.2.2 Controller estimation

To enable simulations over the whole heating period, the control of the radiator has to function without the measured inputs. The supply temperature setpoint for the heat pump is known. However, the actual temperatures fluctuate and decrease before reaching the radiator. So in addition to the set heating curve, heating curve fit from measured supply temperatures was tested.

The thermostat controls the radiator somehow dependent on the room air temperature it measures and its setpoint. PI control is assumed. Several different algorithms are compared where PI parameters are varied, input air and set temperatures modified. There is no measurement point away from the radiator, so the radiator surface temperature compensated air temperature is tested as the air temperature input. It is clear that after some learning period, the radiator introduces pre-heating to reach the given setpoint at given time. Therefore, the setpoint is changed so that the higher levels start earlier. A linear change of the setpoint is also tested.

2.3 Heating period simulations

2.3.1 Input data

The saving potential of the intermittent heating was evaluated on heating period of October 1st to April 30th. Estonian Test Reference Year (TRY) was used for the weather data [7]. Heat recovery ventilation with 80 % efficiency was added to all cases as comparison. The supply air temperature was fixed to 17 °C with balanced air flows of 0.42 l/sm^2. If the ventilation supply temperature were higher than the lower level, the savings would have been less.

The internal gains and temperature setpoints were varied to emulate four different room usage types: living areas, sleeping areas, children's rooms and helping rooms. The usage profiles by hour of the day are shown in Fig. 4.The shown on-off signals represent both when the internal gains from people and the temperature setpoints. The internal gains lower level was zero and the maximum level was defined separately for each profile type and is defined below. The lower setpoint was 18 °C and the higher 21 °C.

Living areas such as living rooms and kitchens are used in the mornings and evenings. In the living areas, the maximum internal gain from people was fixed to 5.3 W/m^2 as in the used residential house there are simultaneously two people in the living areas of 32 m^2 (180 W / 32 m^2 = 5.6 W/m^2). The maximum internal gains from equipment was assumed to be 3 W/m^2 multiplied by the profile given in the Estonian regulation [8] and shown in Fig. 5.

The helping rooms such as corridors, bathrooms, laundry rooms, etc. are called type "extra" in the following. These rooms had same setpoint profiles as living areas. However, these rooms did not include internal gains from people, only the internal gains from equipment.

The sleeping areas are master bedrooms, which are only used at night. The room was assumed to be used by two people so the maximum internal gain was assumed to be 2 x 90 W. Children's rooms are used not only for sleeping but more extensively. Child area was assumed to be for one child, so the internal heat generation maximum was 90 W. For sleeping and children's rooms a variation was tested with cold temperatures allowed during sleep. For children, the lower temperatures were allowed from 9 p.m. to 9 a.m. In the master bedroom this results in constant 18 °C setpoint profile.

2.3.2 Benchmark

The energy saving potential of a defined case was defined as the relative change in the net heating demand compared to the benchmark case. The benchmark case had temperature setpoint constantly at 21°C. The benchmark was different for each case as the internal gains of the compared case were kept.

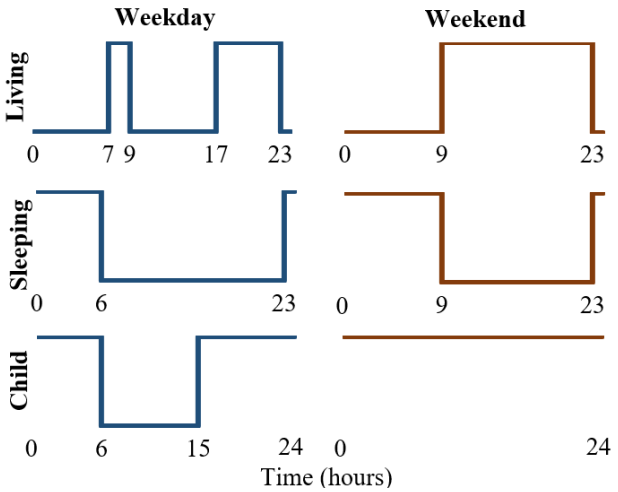

Fig. 4. Defined usage profiles of the different rooms

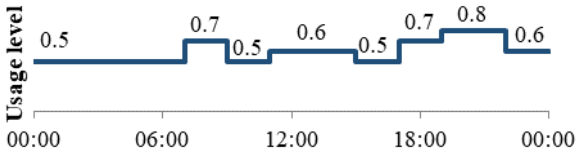

Fig. 5. Equipment usage profile in livng and extra areas

2.3.2 Simulation tests

First, the saving potential was estimated in the test room with adjacent rooms kept at 21 °C. It is clear that the adjacent rooms heat the test room in this case. So the net heating demand was calculated adding up the radiator heat emission and heat fluxes through internal constructions and leaks.

In reality, rooms of different usage are next to each other. So some of the time one room cools down, the adjacent room heats it. Therefore, the resulting saving potential in a whole building would be very different than the savings of different room types added up.

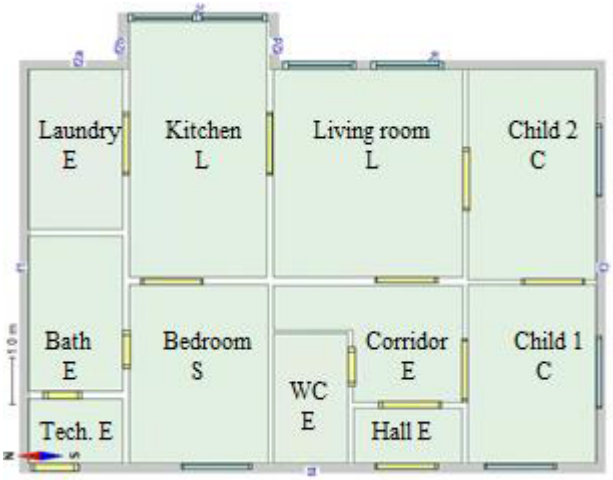

Fig. 6. The floor plan of the simulated residential house, the letters note the usage type applied to the rooms

Table 1. The varied parameters and their values for the calibrated model

	Parameter	Value
Solar gains	Dirtiness of windows (g-value reduction)	40 %
	Transparency of the park	0.3
Internal gains	Internal gains time constant	600 s
	Internal gains convection-radiation split	0.8
Air flows	Leak to outside	0.8 l/s
	Leak to attic	1.2 l/s
	Leak area to Corridor	0.1 m^2
	Leak area to Room 8	0.005 m^2
Radiator heat emission	Heat transfer between radiator and the wall	Only radiative
	Heat transfer coefficient between liquid and the radiator surface	100 W/K
	Heat transfer coefficient between surface and ambient	40 W/K
	Minimum mass flow	1e-4 kg/s
	Maximum mass flow	0.02 kg/s

So secondly, a whole house with a mix of different profiles was simulated. The house is essentially the calibrated test building but the floor plan is adjusted to a more typical residential building. An example of a 100 m^2 one-family house was used, which has been also applied in Estonian guidelines for nearly zero energy buildings and scientific publications before [9, 10]. The room areas were changed from the original to include the test room in the original size for comparisons. Also the orientation remains the one of the test house and the windows as well. Only two windows from the northern facade were shifted to the eastern facade. The resulting floor plan is shown in Fig. 6. The capital letters note the profile types used in these rooms: living L, sleeping S, children C, and extra E. By area the profile types are divided as follows: 34% living, 11% sleeping, 23% children, 31% extra. To compare different profiles both simulated separately and in the mix of profiles, for some cases the bedroom and room child1 were exchanged in their function but not in the areas as the difference in areas is just 1 m^2.

3 Results

3.1 Calibration precision

The parameter values, which resulted in the most accurate air temperatures and mass flows, compared to the measurements, are shown in Table 1. The default IDA ICE water radiator model was changed to the dynamic radiator with mass modelled to get dynamically better results. All radiator parameters that were given by its producer were defined as designed.

As the supply and return temperatures were measured on the pipes, the temperature dropped to room temperature when there was no mass flow. Therefore, for more exact simulation the radiator was turned off while the supply temperatures were below 22 °C. Otherwise, the mass flow was controlled by a PI controller, which tracked the return temperature. Optimizing its control parameters did not improve the results.

The optimal solution reached AAE of 0.25 K. The model was then further used to estimate the control. In this process, the supply temperature was chosen first. One of the heating curves was the setpoint given to the heat pump. The second was the linear model fitted from the measured data at times with significant mass flow (at least 0.015 kg/s). The latter showed AAE of 0.23 K while the first had AAE of 0.37 K. What is more important here, the total radiator heat output during the experiment was 2% higher than the calibrated case for the fitted supply temperature and 12.6 % higher for the setpoint curve. Therefore, the fit temperature curve was further applied. The model was:

$$T_{supply} = -0.6065 \cdot T_{out} + 35.182\ [°C] \qquad (1)$$

The mass flows showed that after some initial learning, the smart thermostat started to heat before the setpoint was actually raised. For the weekday morning high temperature period, it started around 1 to 1.5 hours early, and for the evening peak around 2 to 3 hours early.

However, the times clearly varied from one day to another. The optimal solution was to use a linearly increasing setpoint, which started to raise 1 h early for the morning, and 3 hours early for the evening peak.

The air temperature of the controller also seemed to be something else than measured elsewhere in the room as the controller almost never reached the setpoint. We assumed that at the thermostat the temperature had been higher. We found a correction factor dependent on the radiator surface temperature. Applying the suitable correction factor to the air temperature, we got an indication what temperature the thermostat could have measured:

$$T_{air\_increased} = (T_{surf} - 20)/20 + T_{air}\ [°C] \qquad (2)$$

where Tsurf is the radiator surface temperature 30 s before. Therefore, at 40 °C radiator surface temperature, a 1 K higher air temperature would be measured, and therefore in the center of the room, the temperature would only reach 20 °C instead of 21 °C. However, as both the constant setpoint and variable setpoint cases would behave the same, the setpoints were kept as defined previously.

Finally, the calibrated control model had AAE of 0.27 K, the radiator heat output had increased by 4.4 % from the initial calibration. However, as the heat pump had not reached the set temperatures at the end of the experiment, just changing the supply temperature to the fitted model had increased the heat output by 2 %. The change from there was just 2.4 %.

The air temperatures, mass flows, supply, return and radiator surface temperatures for the measured, calibrated and the calibrated control cases are shown in Fig. 7. We can see that the air temperatures match very well along all the cases but never drop lower than 19 °C. For the calibrated case, also the mass flows and supply and return temperatures fit well to the measurements. For the mass flows, the times when the radiator is turned off, there is some flow measured in the mixing station due to the bypass. This can be omitted for the radiator.

For the calibrated control, mass flows are fluctuating much less than measured. It was attempted to change this situation by varying PI control parameters but unsuccessfully. Due to higher average flows, the return temperature was lower.

The simulated radiator surface temperatures are not fitting that well to the measurements. As in IDA ICE, the convective heat emission of the radiator does not influence the surface temperature, it is clear that these are not exactly the same and do not have to match. The surface temperatures between the calibration and calibrated control match.

Although the total heat emission during the experiment period is very similar between the calibration and calibrated control, the dynamic heat output profile of the calibrated control fluctuates lot less. There are also some imprecision at heating starting and stopping times.

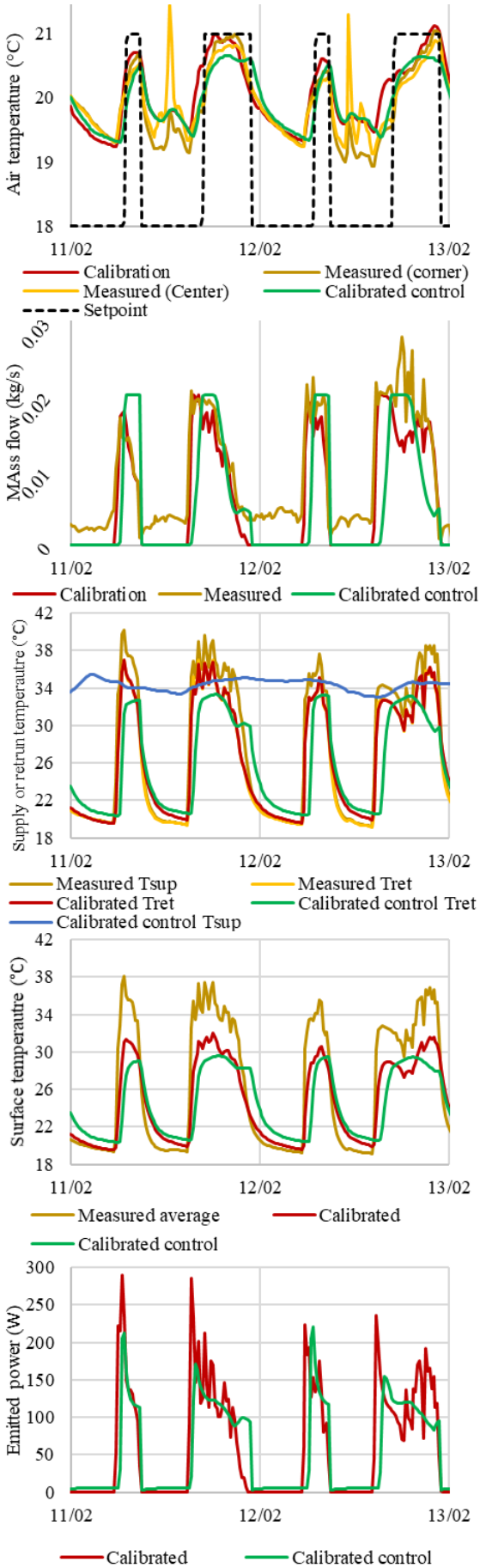

Fig. 7. The calibrated base and calibrated control results compared to the measurements

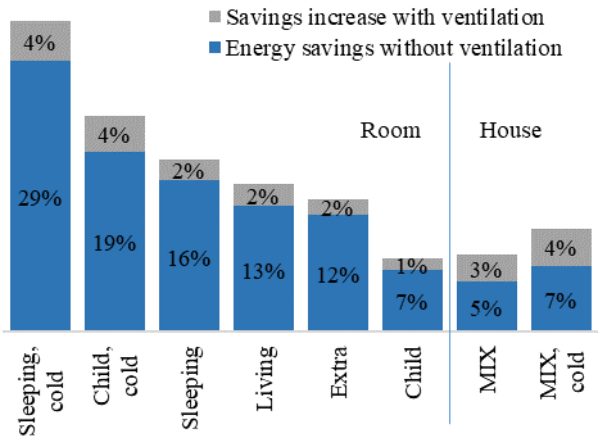

Fig. 8. Energy saving potential for the different profiles with boundaries at 21°C (room) or in the mix of different profiles (house) with and without heat recovery ventilation

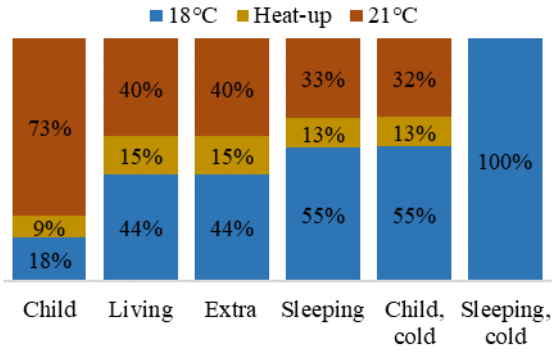

Fig. 9. The share of time the setpoint is high, low, or in-between for the different setpoints

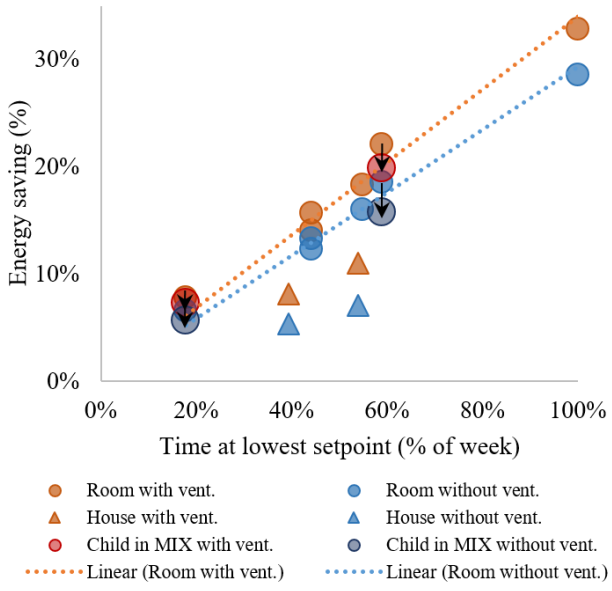

Fig. 10. Energy saving potential dependent on the percent of time the profile has setpoint of 18 °C

3.2 Energy saving potential

The energy saving potential results are shown in Fig. 8. The room-based results on the left show that for the different profiles the energy saving potential ranged from 7 to 29 % for the calibrated control case with no ventilation. When ventilation was added, the savings were 1 to 4 % higher. The whole house profile mix (MIX) cases showed lot lower savings potential, 8 to 11 % with ventilation. Sleeping cold and child cold are the corresponding profile types with night setbacks allowed.

It is clear that the energy saving potential is closely related to the time that lower setpoints are allowed. As the smart thermostat applied some pre-heating, the heat-up process was included in the heating period simulations as well. For most cases, the higher temperature level was kept for a longer period of time than 3 hours, so the 3-hour pre-heating was applied. Only in the case of living areas morning peak, the one-hour heat-up was used. The percentage of the week spent at different setpoint levels or in the pre-heating process are shown in Fig. 9 for all profiles.

Plotted against the percentage of time at setpoint 18 °C (blue columns in Fig. 9), the energy saving potential is visualised in Fig. 10. The room-based results linearly depend on this time. The cases with ventilation depend on it with a steeper rise than the cases without ventilation. As an example, the results for the room Child 1 in the house with a mix of profiles is separated. It can be seen, that the energy saving potential has decreased compared to the case its boundaries are constantly at 21 °C without any additional internal gains raising the temperatures (black arrows indicate the change). The decrease is up to 3 % for this and the sleeping room.

The time at lowest setpoint for the house results is calculated as the area-weighted average of the profiles. The house results have clearly lower energy saving potential than the rooms separately. The cases would still lie lower than the linear lines even if the lowest time percentage over all the profiles in the mix would be used.

In modern homes, air temperature setpoint is often higher than standard 21 °C. To observe its effect on energy saving, two additional cases of the house were simulated. The constant reference situation was raised by 2 °C to 23 °C, all the variable profiles were raised by 2 °C resulting in profiles with lower level at 20 °C and higher at 23 °C. Due to higher gradient to outdoor, the losses would be higher at higher temperatures. However, the heating would have to use more energy to compensate for this. In the 20/23 °C profile case for the MIX with ventilation, energy saving was 7.6 kWh/m^2, which is 6 % of the constant 23 °C. The relative difference is similar to the 8 % saving shown for 18/21 °C above. However, in the 18/21 °C case, the absolute energy saving was 2.2 kWh/m^2. Therefore, the absolute saving at higher temperature profile is clearly higher and the relative saving is a bit lower. The lower relative difference could be caused by the fact that 3 °C setback in the profile makes up smaller proportion of the indoor to outdoor temperature gradient in the higher profile case.

4 Discussion

It was possible to calibrate the measured data very precisely when the radiator supply and return temperatures were known. It was a bigger challenge to find a control algorithm that would explain what the smart thermostat did. However, with the found solution the energy consumption and air temperature were closely matched to the measurements.

As the radiator was measuring lower temperature for air than it was in the centre of the room, the centre almost never reached the setpoint. Usually, a temperature setpoint shift is carried out in such a situation. However, here it was not done as the comparison was relative and the shift should have been applied both to the constant and the variable setpoint.

Not reaching the setpoint temperatures could also be explained by the very low mass flows in the heating system. The system should also be calibrated in a normal functioning case with several radiators to clarify whether the response to changing the setpoints is same in principle.

The variable profiles really have a huge impact, our study shows. However, to get an overview, what the real extents are, a large variety of different profiles should be simulated. A stochastic approach should be applied too but then the logic of the controller has to be known. In this work, a black-box model of the controller was calibrated but these models would vary for different products. For determining the pre-heating times, the pre-heating time was set to constant in most cases. A smart controller could work better than just a fixed period of pre-heating. Moreover, the internal gains are always full loads in this work, but in future works, partial loads should be included as well. In addition to different profiles and gains, the building U-values and heat capacity should be varied as well.

5 Conclusions

The aim of this work was to determine energy saving potential of different usage and setpoint profiles in residential low energy building in a cold climate. It was found that the energy saving potential for the tested profiles ranged from 7 to 33 %. However, when the same profiles were mixed up into the rooms of a single-family house, the energy saving potential was decreased to 8 % saving. In future works, the analysis should be replicated with several different smart thermostats on a variety of realistic buildings with different heat loss and capacity.

This research was supported by the Estonian Centre of Excellence in Zero Energy and Resource Efficient Smart Buildings and Districts, ZEBE (grant No. 2014-2020.4.01.15-0016) and the programme Mobilitas Pluss (Grant No 2014-2020.4.01.16-0024, MOBTP88) funded by the European Regional Development Fund, by the Estonian Research Council (grant No. PSG409) and by the European Commission through the H2020 project Finest Twins (grant No. 856602). We would also like to thank Eesti Energia AS for supplying the thermostats and smart sockets.

References

1. D. Malekpour Koupaei, T. Song, K. S. Cetin, and J. Im, *Build. Environ.*, vol. 170, p. 106603, 2020.
2. U. Ayr *et al.*, *IOP Conf. Ser. Mater. Sci. Eng.*, vol. 609, no. 6, 2019.
3. EQUA, “IDA Indoor Climate and Energy (IDA ICE, version 4.8 SP1, Expert edition).” 2019.
4. M. Maivel, A. Ferrantelli, and J. Kurnitski, *Energy Build.*, vol. 166, pp. 220–228, 2018.
5. T. M. Kull, M. Thalfeldt, and J. Kurnitski, *J. Phys. Conf. Ser.*, vol. 1343, no. 1, 2019.
6. K. V. Võsa, A. Ferrantelli, and J. Kurnitski, *E3S Web Conf.*, vol. 111, no. 201 9, 2019.
7. T. Kalamees and J. Kurnitski, *Proc. Est. Acad. Sci. Eng.*, vol. 12, no. 1, pp. 40–58, 2006.
8. “Estonian Regulation No 58” Ministry of Economic Affairs and Communications, 2015.
9. R. Simson, E. Arumägi, K. Kuusk, and J. Kurnitski, *E3S Web Conf.*, vol. 111, no. 201 9, 2019.
10. Tallinn University of Technology, 2017. [Online]. Available: https://kredex.ee/sites/default/files/2019-03/Liginullenergia_eluhooned_Vaikemaja_juhend.pdf. [Accessed: 03-Apr-2020].